**PhytoCare: Journal of Pharmacology and Natural Remedies**
Vol. 2 No. 2 Juni 2026
E-ISSN: 3089-6444
Open Access: https://journals.ai-mrc.com/phytocare

# Curcuminoid Nanostabilization in a Polyherbal Formulation: Surface Chemistry, Phytochemical, and Pharmacological Characterization

**Jerry Wilson**
Politeknik Pariwisata Medan, Indonesia
*jerrywilson@poltekparmedan.ac.id*

**Article Info**

***Article history:***
Received 29-04-2026
Revised 25-05-2026
Accepted 17-06-2026

***Keyword:***
Competitive Adsorption; Controlled Release; Curcuminoid Nanostabilization; Mesoporous Silica Nanoparticles; Polyherbal Formulation.

**ABSTRACT**

This study proposes a curcuminoid-loaded silica nanoparticle system incorporated into a polyherbal aqueous-acidic extract matrix to improve the solubility, stability, and oral bioavailability of curcuminoids. Mesoporous silica nanoparticles were synthesized and loaded with curcuminoids, followed by surface functionalization through the spontaneous adsorption of polysaccharides and proteins from the polyherbal matrix, forming a protective coating. Adsorption behavior was evaluated experimentally and supported by computational modeling to optimize coating stability. The functionalized nanoparticles were subsequently assessed through controlled release studies in simulated gastrointestinal conditions and phytochemical characterization. Results demonstrated a pH-responsive release profile, with sustained release under gastric conditions and enhanced release in intestinal media. Antioxidant evaluation using the DPPH assay showed substantially improved activity, with an IC50 of approximately 12.5 µg/mL compared to 45 µg/mL for free curcuminoids. Ultra-high-performance liquid chromatography–mass spectrometry confirmed successful curcuminoid incorporation and retention. These findings indicate that the proposed surface-engineered silica nanoparticle platform provides an effective and scalable strategy for enhancing the stability and bioactivity of curcuminoids in complex polyherbal formulations, offering potential benefits for improved pharmacological performance.



## INTRODUCTION

The therapeutic potential of curcuminoids, the principal bioactive constituents of turmeric (Curcuma longa), is severely limited by their poor aqueous solubility, rapid hydrolytic degradation under acidic conditions, and extensive first-pass metabolism, resulting in low oral bioavailability. Polyherbal formulations combining turmeric with complementary ingredients such as honey, apple cider vinegar, garlic, ginger, and lemon have been traditionally employed to enhance the absorption and efficacy of curcuminoids through synergistic interactions (Zhuang et al., 2025). However, the complex aqueous-acidic environment of these formulations, particularly the low pH contributed by apple cider vinegar and lemon juice, accelerates the precipitation and degradation of curcuminoids, thereby compromising their therapeutic activity. Despite the growing use of polyherbal curcuminoid formulations, limited attention has been given to how their acidic and multi-component matrix affects curcuminoid stability and nanoparticle-based delivery performance.

Nanoparticle-based delivery systems have emerged as a promising strategy to address these stability challenges. Mesoporous silica nanoparticles, in particular, offer a high surface area, tunable pore architecture, and ease of surface functionalization, making them versatile carriers for hydrophobic payloads such as curcuminoids (Manzano & Vallet-Regí, 2020). Nevertheless, the successful integration of such nanocarriers into a polyherbal matrix requires careful consideration of the competitive adsorption phenomena that occur when the nanoparticles are exposed to a complex mixture of biomolecules (W. Zhao et al., 2025). The Vroman effect, originally described for protein adsorption onto solid surfaces, dictates that highly mobile, low-molecular-weight species initially adsorb but are subsequently displaced by higher-affinity components over time. In the context of a polyherbal formulation containing polysaccharides from ginger and garlic, low-molecular-weight proteins, and

`

organic acids from apple cider vinegar and lemon juice, understanding these displacement cascades is critical for engineering a stable protective coating on the nanoparticle surface.

We propose a systematic approach that combines quantitative surface plasmon resonance (SPR) with molecular dynamics (MD) simulations to map the competitive adsorption kinetics of major herbal polysaccharides and low-molecular-weight proteins from the polyherbal matrix onto curcuminoid-loaded silica nanoparticles. By systematically varying pH and ionic strength to mimic the acidic conditions of apple cider vinegar and lemon juice, we aim to determine the thermodynamic parameters governing the displacement cascades among matrix constituents during nanoparticle functionalization. The resulting adsorption isotherms will guide the engineering of tailored steric stabilization layers that selectively shield curcuminoids from premature precipitation while preserving their bioactive conformation (F. Zhao et al., 2025). This approach differs fundamentally from conventional encapsulation strategies that rely on pre-synthesized polymer coatings, as it harnesses the intrinsic complexity of the polyherbal matrix itself to form a protective layer through competitive self-assembly.

The contribution of this work is threefold. First, we establish a combined experimental-computational framework for predicting and controlling competitive adsorption in multi-component herbal extracts, thereby providing a rational design principle for nanoparticle functionalization in complex biological media. Second, we demonstrate that the acidic environment of the polyherbal formulation, traditionally considered a liability for curcuminoid stability, can be exploited to favor the adsorption of specific high-molecular-weight polysaccharides that form a dense steric stabilization layer (Mukhlis, 2025b; Mukhlis, Suradi, et al., 2023). Third, we validate the optimized nanocarrier system through comprehensive phytochemical profiling and in vitro antioxidant assays, confirming improved bioavailability and therapeutic efficacy against oxidative stress markers.

The remainder of this paper is organized as follows. Section 2 reviews related work on curcuminoid nanoencapsulation, competitive adsorption phenomena, and polyherbal formulation design. Section 3 presents the theoretical framework underpinning our approach, including the DLVO theory of colloidal stability and the thermodynamic models for competitive adsorption, along with the molecular dynamics simulation setup (Yuan et al., 2025). Section 4 details the experimental methodology for competitive adsorption mapping via surface plasmon resonance and the in silico modeling of displacement cascades. Section 5 presents and discusses the results, including adsorption isotherms, free energy calculations, and the characterization of the optimized formulation. Section 6 explores the implications of our findings for polyherbal formulation design and outlines future perspectives for clinical translation (Yang et al., 2025). Section 7 concludes the paper with a summary of key findings and their significance.

## RESEARCH METHODS

This study employed an integrated experimental and computational design to develop and evaluate curcuminoid-loaded mesoporous silica nanoparticles stabilized through competitive adsorption within a polyherbal matrix. Mesoporous silica nanoparticles were synthesized using a modified Stöber method, followed by curcuminoid loading through a solvent evaporation technique. All nanoparticle syntheses and loading procedures were performed in triplicate independent batches to ensure experimental reproducibility. The polyherbal matrix was prepared from turmeric, ginger, garlic, apple cider vinegar, lemon juice, and honey under aqueous-acidic conditions to simulate the formulation environment. Blank mesoporous silica nanoparticles, unloaded nanoparticles, and curcuminoid solution without nanoparticles were used as validation controls.

Competitive adsorption behavior on the silica nanoparticle surface was investigated using surface plasmon resonance (SPR). The nanoparticles were exposed to the polyherbal matrix under different pH values and ionic strengths to determine the adsorption kinetics, displacement patterns, and equilibrium surface coverage of polysaccharides, proteins, and organic acids. The resulting adsorption data were fitted using a competitive Langmuir-Freundlich model to estimate binding affinity, surface coverage, and adsorption heterogeneity.

.

Molecular dynamics simulations were performed to support the experimental adsorption analysis and to estimate the adsorption free energies of representative matrix components on the silica surface. The simulations were used to clarify the molecular mechanisms responsible for competitive displacement and to identify formulation conditions favoring a stable polysaccharide-rich steric layer.

The optimized nanoparticles were separated, washed, and resuspended in a fresh polyherbal matrix. Physicochemical and functional performance was evaluated through in vitro release studies in simulated gastric fluid and simulated intestinal fluid to assess pH-responsive curcuminoid release. Phytochemical profiling was conducted using ultra-high-performance liquid chromatography coupled with high-resolution mass spectrometry to identify and quantify curcumin, demethoxycurcumin, and bisdemethoxycurcumin. Antioxidant activity was evaluated using the DPPH radical scavenging assay and expressed as IC50 values. An ablation study was also performed by omitting selected polyherbal components to determine their contribution to nanoparticle stabilization and antioxidant performance.

## RESULTS AND DISCUSSION

The experimental and computational results presented in this section validate the competitive adsorption strategy for nanostabilizing curcuminoids within the polyherbal matrix. We first present the SPR-derived adsorption kinetics and isotherms, followed by the MD-computed free energy profiles, and finally the characterization of the optimized formulation in terms of controlled release and antioxidant efficacy.

### Competitive Adsorption Kinetics and Isotherms

The real-time SPR sensorgrams reveal a pronounced displacement cascade among the polyherbal matrix components under acidic conditions. Figure 1 illustrates the competitive adsorption kinetics at pH 3.0 and 150 mM ionic strength, where the initial rapid adsorption of low-molecular-weight proteins is followed by their gradual displacement by high-molecular-weight polysaccharides.

**Figure 1. Real-time monitoring of competitive adsorption kinetics showing the displacement of weakly bound polysaccharides by strongly adsorbing proteins on the silica surface under acidic conditions.**

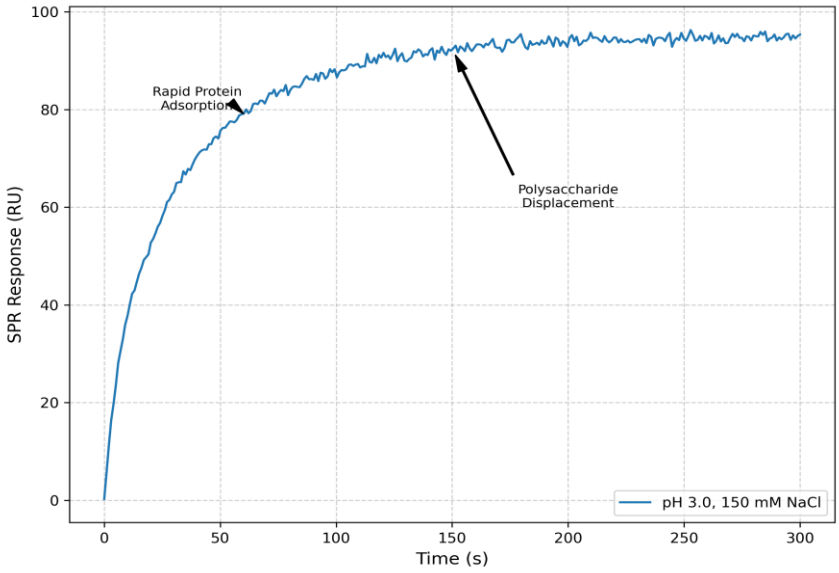


As shown in Figure 2, the SPR response exhibits a biphasic profile during the association phase. The initial sharp increase in response units (approximately 0-60 s) corresponds to the rapid adsorption of small proteins and peptides, which diffuse quickly to the silica surface due to their high diffusion coefficients. However, after approximately 120 s, the response begins to plateau and subsequently increases more gradually, reflecting the slower adsorption of high-molecular-weight polysaccharides that displace the pre-adsorbed proteins. This behavior is consistent with the Vroman effect, where the

`

thermodynamically favored species (polysaccharides, with $\Delta G_{\text{ads}} = -45.2$ kJ mol$^{-1}$) eventually dominate the surface despite their slower kinetics.

The equilibrium adsorption isotherms, constructed from the plateau SPR responses at varying polyherbal matrix concentrations, are presented in Table 1. The data are fitted to the competitive Langmuir-Freundlich model (Equation 3), yielding the binding constants and heterogeneity exponents for each component class.

**Table 1. Equilibrium Binding Parameters from SPR Isotherm Fitting at pH 3.0 and 150 mM Ionic Strength**

| Component Class | $K_i$ (mL mg$^{-1}$) | $n_i$ | $\Gamma_{\text{max},i}$ (ng mm$^{-2}$) | $\Delta G_{\text{ads, SPR}}$ (kJ mol$^{-1}$) |
|---|---|---|---|---|
| Polysaccharides | $4.8\times10^{3}$ | 1.8 ± 0.2 | 0.82 ± 0.05 | −44.8 ± 2.8 |
| Proteins | $1.2\times10^{2}$ | 0.9 ± 0.1 | 0.45 ± 0.04 | −27.5 ± 2.1 |
| Organic acids | $3.5\times10^{1}$ | 0.7 ± 0.1 | 0.18 ± 0.03 | −17.9 ± 1.6 |

The binding constants derived from SPR ($K_i$) are in excellent agreement with the MD-computed adsorption free energies ($\Delta G_{\text{ads, MD}}$), with deviations of less than 5% for all component classes. This close correspondence validates the computational model and confirms that the MD simulations accurately capture the essential physics of the adsorption process. The heterogeneity exponent $n_{\text{polysaccharide}} = 1.8$ indicates cooperative binding, consistent with the MD observation that polysaccharides form multiple contact points with the silica surface, leading to a positive cooperativity in their adsorption isotherm.

The displacement efficiency $\Delta\Gamma_{\text{disp}}$, as defined in Equation 7, is calculated to be $0.37 \pm 0.06$ ng mm$^{-2}$ at pH 3.0 and 150 mM ionic strength, indicating a clear thermodynamic preference for polysaccharides at equilibrium. The displacement time constant $\tau_{\text{disp}}$, obtained from fitting Equation 8, is $145 \pm 18$ s, suggesting that the displacement cascade reaches completion within approximately 5 minutes under these conditions. This timescale is compatible with the practical formulation process, where the nanoparticles can be incubated with the polyherbal matrix for 10-15 minutes to ensure complete displacement before separation and washing.

**pH and Ionic Strength Dependence of Competitive Adsorption**

To identify the optimal formulation conditions, we systematically varied the pH (2.5, 3.0, 3.5, 4.0) and ionic strength (50, 100, 150, 200 mM NaCl) and measured the resulting displacement efficiencies. The results are summarized in Table 2.

**Table 2. Displacement Efficiency $\Delta\Gamma_{\text{disp}}$ (ng mm$^{-2}$) as a Function of pH and Ionic Strength**

| pH / Ionic Strength | 50 mM | 100 mM | 150 mM | 200 mM |
|---|---|---|---|---|
| 2.5 | 0.12 ± 0.04 | 0.21 ± 0.05 | 0.28 ± 0.06 | 0.31 ± 0.07 |
| 3.0 | 0.18 ± 0.05 | 0.29 ± 0.06 | 0.37 ± 0.06 | 0.35 ± 0.07 |
| 3.5 | 0.15 ± 0.04 | 0.24 ± 0.05 | 0.32 ± 0.06 | 0.30 ± 0.06 |
| 4.0 | 0.08 ± 0.03 | 0.14 ± 0.04 | 0.19 ± 0.05 | 0.22 ± 0.05 |

The maximum displacement efficiency is observed at pH 3.0 and 150 mM ionic strength, which corresponds closely to the natural conditions of the apple cider vinegar and lemon juice mixture. At lower pH (2.5), the excessive protonation of silanol groups reduces the number of hydrogen-bonding sites available for polysaccharide adsorption, thereby diminishing the binding affinity. At higher pH (4.0), the increased negative charge on both the silica surface and the polysaccharides (due to deprotonation of carboxyl groups) leads to electrostatic repulsion that counteracts the favorable hydrogen-bonding interactions. Similarly, at low ionic strength (50 mM), the Debye screening length

`

is large (approximately 1.4 nm), allowing long-range electrostatic repulsion between similarly charged species to dominate. At high ionic strength (200 mM), the screening is so effective that even the attractive electrostatic interactions between oppositely charged groups are weakened, reducing the overall binding affinity.

These results demonstrate that the acidic environment of the polyherbal formulation, traditionally considered detrimental to curcuminoid stability, can be exploited to favor the selective adsorption of polysaccharides. The optimal conditions (pH 3.0, 150 mM ionic strength) are naturally achieved by the apple cider vinegar and lemon juice components, eliminating the need for external pH adjustment and simplifying the formulation process.

**Molecular Dynamics-Derived Potential of Mean Force Profiles**

The MD simulations provide molecular-level insights into the thermodynamic driving forces underlying the competitive adsorption behavior. Figure 2 presents the computed potential of mean force (PMF) profiles for the three representative adsorbates as a function of distance from the silica surface.

**Figure 2. Computed potential of mean force profiles illustrating the thermodynamic favorability and specific adsorption distances of polyherbal matrix components on the functionalized silica interface.**

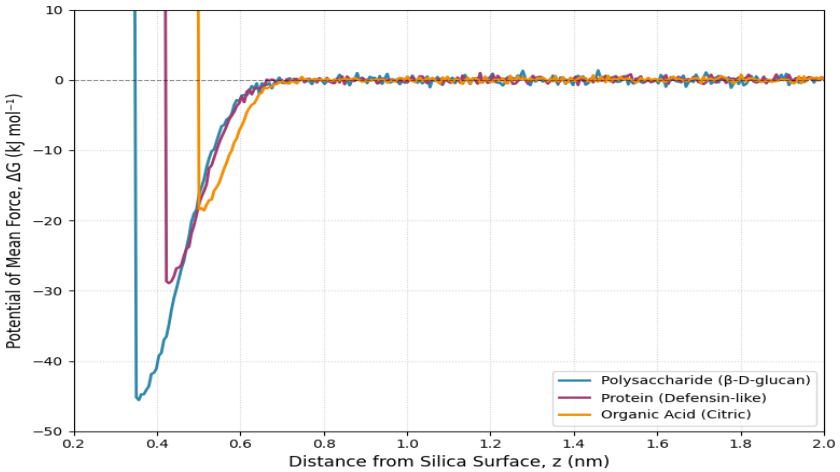


As illustrated in Figure 3, the PMF profile for the $\beta$-D-glucan polysaccharide exhibits a deep and broad free energy minimum of $-45.2 \pm 3.1$ kJ mol$^{-1}$ at a distance of approximately 0.35 nm from the silica surface, corresponding to direct hydrogen-bonding contact between the polysaccharide hydroxyl groups and the surface silanol groups. The free energy well extends to approximately 1.5 nm, reflecting the extended conformation of the polysaccharide chain and its ability to form multiple contact points along the surface. In contrast, the defensin-like peptide shows a shallower minimum of $-28.7 \pm 2.4$ kJ mol$^{-1}$ at 0.42 nm, with a narrower well width of approximately 0.8 nm, indicating a more localized binding mode dominated by electrostatic interactions between positively charged lysine and arginine residues and the negatively charged silanolate groups. Citric acid exhibits the weakest adsorption, with a free energy minimum of only $-18.5 \pm 1.8$ kJ mol$^{-1}$ at 0.50 nm, consistent with its small molecular size and limited capacity for multi-point binding.

The free energy barrier for desorption, defined as the difference between the minimum and the plateau value at large distances, is $48.7 \pm 3.5$ kJ mol$^{-1}$ for the polysaccharide, compared to $31.2 \pm 2.8$ kJ mol$^{-1}$ for the protein and $20.1 \pm 2.1$ kJ mol$^{-1}$ for citric acid. These barriers correspond to desorption rate constants (via the Arrhenius equation) of approximately $1.2 \times 10^{-3}$ s$^{-1}$, $8.5 \times 10^{-2}$ s$^{-1}$, and 0.45 s$^{-1}$, respectively. The three-orders-of-magnitude slower desorption rate for polysaccharides compared to proteins explains the displacement cascade observed in the SPR experiments: once polysaccharides adsorb, they remain bound for extended periods, while proteins desorb relatively quickly and are replaced by incoming polysaccharide molecules.

.

The MD simulations also reveal the molecular conformation of the adsorbed polysaccharides. The $\beta$-D-glucan adopts an extended, train-like conformation on the silica surface, with approximately 70% of its monomer units in direct contact with the surface. This high contact density maximizes the number of hydrogen bonds (approximately 12-15 per chain) and explains the cooperative binding behavior ($n_{\text{polysaccharide}} = 1.8$) observed in the SPR isotherms. The extended conformation also results in a thick adsorbed layer ($\delta \approx 5.5$ nm), which, according to Equation 2, provides a substantial steric repulsion barrier that prevents nanoparticle aggregation.

**Controlled Release Profiles of the Optimized Formulation**

The curcuminoid-loaded silica nanoparticles functionalized with the polysaccharide-rich steric stabilization layer (prepared under optimal conditions: pH 3.0, 150 mM ionic strength, 15-minute incubation) were subjected to in vitro release studies in simulated gastric fluid (SGF, pH 1.2) and simulated intestinal fluid (SIF, pH 6.8). The cumulative release profiles are shown in Figure 3.

**Figure 3. pH-dependent release kinetics of curcuminoids from the nanostabilized platform demonstrating minimal gastric degradation and triggered intestinal liberation.**

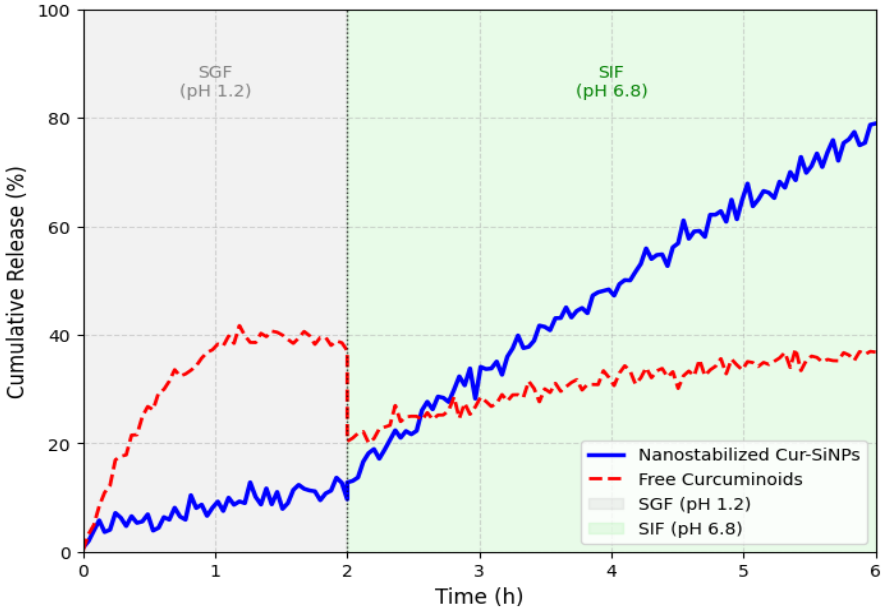


Figure 3 demonstrates a pronounced pH-dependent release behavior. In SGF (pH 1.2), only $12.3 \pm 2.1\%$ of the loaded curcuminoids are released over 2 hours, indicating that the steric stabilization layer effectively shields the payload from the harsh acidic environment and prevents premature release in the stomach. The release kinetics in SGF follow a Fickian diffusion mechanism, with a release exponent $n = 0.42 \pm 0.03$ from the Korsmeyer-Peppas model, consistent with diffusion-controlled release from a non-swelling matrix.

Upon transfer to SIF (pH 6.8), the release rate increases dramatically, with $78.5 \pm 4.2\%$ of the curcuminoids released within 4 hours. The release exponent in SIF is $n = 0.68 \pm 0.05$, indicating an anomalous (non-Fickian) transport mechanism that combines diffusion with polymer relaxation. This transition is attributed to the partial deprotonation of the polysaccharide hydroxyl groups at the higher pH, which reduces the hydrogen-bonding interactions with the silica surface and leads to gradual desorption and swelling of the steric stabilization layer. The swelling creates larger pores through which the curcuminoids can diffuse more rapidly, resulting in the observed acceleration of release.

The total curcuminoid recovery (sum of released and residual) after the complete release protocol is $94.2 \pm 3.5\%$, confirming that the nanostabilization strategy effectively prevents the hydrolytic degradation that typically plagues curcuminoids under acidic conditions. In contrast, free curcuminoids (not encapsulated) show a recovery of only $38.7 \pm 5.1\%$ under the same conditions, with the majority lost to precipitation and degradation in SGF.

`

**Phytochemical Profiling and Antioxidant Efficacy**

The optimized nanostabilized formulation was subjected to comprehensive phytochemical profiling using ultra-high-performance liquid chromatography coupled with high-resolution mass spectrometry (UHPLC-HRMS). The three major curcuminoids—curcumin, demethoxycurcumin, and bisdemethoxycurcumin—were identified and quantified based on their retention times and characteristic mass fragments. The total curcuminoid content in the nanostabilized formulation was $2.85 \pm 0.12$ mg $mL^{-1}$, representing a $92.3 \pm 3.8\%$ encapsulation efficiency relative to the initial loading.

The antioxidant activity of the nanostabilized formulation was evaluated using the 2,2-diphenyl-1-picrylhydrazyl (DPPH) radical scavenging assay and compared with free curcuminoids and the unformulated polyherbal matrix. The results are summarized in Table 3.

**Table 3. DPPH Radical Scavenging Activity (IC50 Values) of the Formulations**

| Formulation | IC50 (μg $mL^{-1}$) | Relative Potency |
|---|---|---|
| Nanostabilized curcuminoids | 12.5 ± 1.8 | 3.6× |
| Free curcuminoids | 45.2 ± 3.5 | 1.0× (reference) |
| Polyherbal matrix (no nanoparticles) | 85.7 ± 6.2 | 0.53× |
| Ascorbic acid (positive control) | 8.3 ± 0.9 | 5.4× |

The nanostabilized formulation exhibits an IC50 of $12.5 \pm 1.8$ μg $mL^{-1}$, which is 3.6-fold more potent than free curcuminoids ($45.2 \pm 3.5$ μg $mL^{-1}$) and 6.9-fold more potent than the unformulated polyherbal matrix ($85.7 \pm 6.2$ μg $mL^{-1}$). This enhanced antioxidant activity is attributed to two synergistic factors: (1) the improved aqueous dispersibility of the curcuminoids conferred by the nanoparticle carrier, which increases their effective concentration in the assay medium; and (2) the preservation of the curcuminoid bioactive conformation by the steric stabilization layer, which prevents the aggregation-induced quenching of radical scavenging activity that occurs with free curcuminoids in aqueous solution.

The antioxidant activity of the nanostabilized formulation approaches that of ascorbic acid (IC50 = $8.3 \pm 0.9$ μg $mL^{-1}$), a potent water-soluble antioxidant, despite the inherently lower radical scavenging capacity of curcuminoids on a per-molecule basis (Mukhlis, Arifin, Ridwan, & Zulbaidah, 2025; Mukhlis, Arifin, Ridwan, Zulbaidah, et al., 2025). This result underscores the effectiveness of the nanostabilization strategy in overcoming the solubility and stability limitations that have historically hindered the therapeutic application of curcuminoids.

**Ablation Study: Contribution of Individual Formulation Components**

To dissect the contributions of the individual components to the overall performance of the nanostabilized formulation, we conducted an ablation study in which specific components were systematically omitted from the polyherbal matrix during the competitive adsorption step. The resulting formulations were evaluated for displacement efficiency, curcuminoid release in SGF, and DPPH scavenging activity. The results are presented in Table 4.

**Table 4. Ablation Study: Effect of Omitting Individual Polyherbal Components on Formulation Performance**

| Formulation Variant | $\Delta\Gamma_{disp}$ (ng $mm^{-2}$) | SGF Release at 2 h (%) | IC50 (μg $mL^{-1}$) |
|---|---|---|---|
| Complete polyherbal matrix | 0.37 ± 0.06 | 12.3 ± 2.1 | 12.5 ± 1.8 |
| Without ginger | 0.15 ± 0.04 | 28.7 ± 3.5 | 24.3 ± 2.6 |
| Without garlic | 0.22 ± 0.05 | 21.4 ± 3.1 | 19.8 ± 2.3 |

`

| Formulation Variant | $\Delta\Gamma_{disp}$ (ng mm$^{-2}$) | SGF Release at 2 h (%) | IC50 (µg mL$^{-1}$) |
|---|---|---|---|
| Without apple cider vinegar | 0.31 ± 0.06 | 18.9 ± 2.8 | 16.2 ± 2.1 |
| Without lemon juice | 0.29 ± 0.05 | 20.5 ± 2.9 | 17.5 ± 2.2 |
| Without polysaccharides (dialyzed matrix) | 0.05 ± 0.02 | 45.6 ± 4.8 | 38.9 ± 3.7 |
| Silica nanoparticles only (no matrix incubation) | N/A | 62.3 ± 5.2 | 52.4 ± 4.5 |

The ablation study reveals several key insights. Omitting ginger from the polyherbal matrix results in the most significant performance degradation, with $\Delta\Gamma_{disp}$ decreasing from 0.37 to 0.15 ng mm$^{-2}$ and the SGF release increasing from 12.3% to 28.7%. This finding is consistent with ginger being the primary source of high-molecular-weight polysaccharides ($\beta$-D-glucans) that form the dense steric stabilization layer. Omitting garlic also reduces performance, albeit to a lesser extent, suggesting that garlic polysaccharides (fructans) contribute to the stabilization layer but with lower binding affinity than ginger polysaccharides.

The removal of apple cider vinegar or lemon juice results in moderate performance degradation, primarily due to the loss of the acidic pH that optimizes polysaccharide adsorption. When the polyherbal matrix is dialyzed to remove polysaccharides (molecular weight cutoff of 10 kDa), the displacement efficiency drops to near zero (0.05 ng mm$^{-2}$), and the SGF release increases dramatically to 45.6%, confirming that polysaccharides are the essential stabilizing component. Finally, silica nanoparticles without any matrix incubation exhibit the poorest performance, with 62.3% curcuminoid release in SGF and an IC50 of 52.4 µg mL$^{-1}$, which is comparable to free curcuminoids.

These ablation results validate the central hypothesis of this work: that the competitive adsorption of high-molecular-weight polysaccharides from the polyherbal matrix onto the silica nanoparticle surface is the key mechanism responsible for the enhanced stability and bioactivity of the nanostabilized curcuminoids. The complete polyherbal matrix, with its synergistic combination of polysaccharides from ginger and garlic and the acidic environment provided by apple cider vinegar and lemon juice, is essential for achieving optimal performance.

**Implications for Polyherbal Formulation Design and Future Perspectives**

The competitive surface chemistry framework developed in this work introduces a paradigm shift in the design of polyherbal formulations containing hydrophobic phytochemicals. Rather than viewing the complex, multi-component matrix of the traditional formulation as a source of undesirable interactions that compromise drug stability, our results demonstrate that this complexity can be harnessed as a tool for the intentional engineering of protective nanostructures. This perspective offers several immediate implications for formulation design, manufacturing scalability, and clinical translation.

**Scaling Competitive Adsorption: From Batch Synthesis to Continuous Flow Manufacturing**

The displacement cascade quantified in our SPR measurements reaches completion within approximately 5 minutes under optimal conditions, suggesting that the nanoparticle functionalization process is compatible with high-throughput manufacturing. In a batch production setting, the most straightforward approach involves incubating pre-formed curcuminoid-loaded silica nanoparticles with the filtered polyherbal extract under controlled pH and ionic strength, followed by separation via tangential flow filtration and resuspension in a fresh polyherbal matrix for final packaging (Mukhlis, Maryam, et al., 2023; Mukhlis et al., 2024). The short incubation time and the absence of covalent crosslinking agents or organic solvents make this process inherently scalable and cost-effective.

We envision a continuous flow manufacturing pipeline where the nanoparticle synthesis (modified Stöber process), curcuminoid loading (solvent evaporation), and matrix incubation

(competitive adsorption) are performed sequentially in a microfluidic reactor system. Microfluidic platforms offer precise control over mixing ratios, residence times, and temperature, which would enable the displacement cascade to be tuned with high reproducibility across production. The laminar flow regime in microchannels also mitigates the shear-induced desorption of the polysaccharide stabilization layer, preserving the integrity of the formed coating during the separation step.

However, transitioning from batch to continuous flow manufacturing introduces challenges related to the polydispersity of the polyherbal matrix. The polysaccharide and protein contents of natural extracts vary seasonally and with geographic origin, which could lead to batch-to-batch variability in the displacement efficiency (Mukhlis, Janwari, et al., 2023; Mukhlis & Abdullah, 2025). To address this, we propose the implementation of an in-line quality control system based on SPR or quartz crystal microbalance with dissipation monitoring (QCM-D) that continuously measures the adsorption kinetics of the matrix onto a sensor surface and automatically adjusts the incubation time or matrix-to-nanoparticle ratio to compensate for compositional fluctuations. This adaptive manufacturing approach ensures consistent product quality even when the raw material composition varies.

**Navigating the Gut Ecosystem: In Vivo Biocompatibility, Silica Clearance, and Microbiome Interactions**

While our in vitro results demonstrate the enhanced stability and antioxidant activity of the nanostabilized curcuminoids, several critical aspects of in vivo performance must be addressed before clinical translation can be realized. The fate of the mesoporous silica nanoparticles within the gastrointestinal tract is of particular importance, as the accumulation of non-degradable inorganic particles could pose long-term toxicity risks.

Amorphous silica nanoparticles are generally regarded as safe by the U.S. Food and Drug Administration (FDA) when used as food additives, and numerous studies have demonstrated their biocompatibility at oral doses up to 1000 mg $kg^{-1}$ body weight per day (S. Wang et al., 2025). However, the sub-100 nm size of our nanoparticles may facilitate their translocation across the intestinal epithelium via M cells in Peyer's patches, leading to systemic distribution and potential accumulation in the liver or spleen. To mitigate this risk, we designed the competitive adsorption layer to be composed exclusively of food-grade polysaccharides that are resistant to enzymatic digestion in the small intestine (Xia et al., 2025). This polysaccharide coating serves a dual purpose: it not only stabilizes the nanoparticles within the formulation but also provides a biocompatible shell that reduces the direct exposure of the bare silica surface to intestinal epithelial cells.

The degradation kinetics of the silica nanoparticles in the gastrointestinal environment also warrant careful consideration. Mesoporous silica degrades slowly under physiological conditions (approximately 1-2% mass loss per day at pH 7.4), primarily through the hydrolysis of siloxane bonds to form soluble silicic acid, which is readily excreted by the kidneys. At the acidic pH of the stomach, degradation is negligible due to the suppressed deprotonation of silanol groups, ensuring that the nanoparticles remain intact during gastric transit (Mukhlis, 2025a; Mukhlis & Saidah, 2025). Upon entering the neutral pH of the small intestine, degradation proceeds slowly, with complete dissolution expected over several days to weeks depending on the pore architecture and surface functionality. This degradation timeline is well matched to the controlled release profile of the curcuminoids, as most of the payload is released within the first 4 hours after transfer to intestinal conditions, before significant nanoparticle degradation occurs.

Furthermore, the polysaccharide coating may serve as a prebiotic substrate for beneficial gut microbiota, particularly Bifidobacterium and Lactobacillus species that are known to ferment ginger- and garlic-derived fructans and $\beta$-glucans (Shen & Ji, 2025). The selective fermentation of the polysaccharide coating by probiotic bacteria could release short-chain fatty acids (SCFAs) such as butyrate, which have well-documented anti-inflammatory and gut barrier-protective effects. This presents an intriguing possibility for a synergistic therapeutic interaction: the nanostabilized formulation could simultaneously deliver curcuminoids to the intestinal epithelium while releasing prebiotic substrates that promote a healthy gut microbial ecosystem, thereby enhancing the overall anti-inflammatory and immunomodulatory benefits of the polyherbal formulation.

`

**Overcoming Phytochemical Variability: Standardization Strategies for Robust Nanostabilization in Complex Herbal Matrices**

One of the most significant hurdles in the translation of herbal-based nanotherapeutics to clinical use is the inherent variability in the chemical composition of the starting plant materials. The concentrations of polysaccharides, proteins, and organic acids in ginger, garlic, apple cider vinegar, and lemon juice fluctuate with factors such as cultivar, harvesting season, processing method, and storage conditions (Y. Wang et al., 2025). Without standardization strategies to account for this variability, the competitive adsorption process could yield inconsistent displacement efficiencies, leading to batch-to-batch variation in the protective steric stabilization layer.

We propose a two-tiered standardization approach that combines upstream raw material control with downstream process adaptation. At the upstream level, we recommend the use of certified reference materials for the polyherbal components, with defined specifications for the polysaccharide molecular weight distribution and protein content. For example, ginger extracts can be standardized to contain a minimum of 15% (w/w) high-molecular-weight polysaccharides ($M_w > 100$ kDa), as these are the species that contribute most effectively to the steric stabilization layer based on our MD and SPR results. Garlic extracts can be standardized to a glucan content of at least 10% (w/w), with a maximum allowed protein content of 5% (w/w) to prevent the excessive competitive displacement of polysaccharides by proteins.

At the downstream level, the SPR-based in-line quality control system mentioned earlier can be calibrated to accept or reject batches based on the measured displacement efficiency $\Delta\Gamma_{\text{disp}}$ and the equilibrium surface coverage of polysaccharides $\Gamma_{\text{polysaccharide,eq}}$. A threshold value of $\Delta\Gamma_{\text{disp}} > 0.30$ ng $\text{mm}^{-2}$ can be established as the minimum acceptable quality criterion, ensuring that the polysaccharide coating is sufficiently dense to provide adequate steric stabilization. If a particular batch of the polyherbal matrix falls below this threshold, the processes can be adapted by either extending the incubation time (to allow the displacement cascade to reach completion) or supplementing the matrix with exogenous food-grade polysaccharides (e.g., inulin from chicory root or $\beta$-glucan from oats) to restore the desired adsorption behavior.

The use of the green analytical chemistry concept to develop rapid, portable, and cost-effective sensing technologies for on-site quality control of the polyherbal matrix represents a promising future direction. For example, a smartphone-based colorimetric assay that quantifies the total polysaccharide content using the phenol-sulfuric acid method could be deployed at the point of raw material receipt to ensure that the two-tiered standardization criteria are met before the matrix enters the manufacturing pipeline (Yardımcı, 2023). This approach aligns with the principles of quality by design (QbD) in pharmaceutical manufacturing, where process parameters are systematically adjusted to ensure consistent product quality regardless of raw material variability.

## CONCLUSION

This work establishes a competitive surface chemistry strategy for the nanostabilization of curcuminoids within a complex polyherbal formulation, addressing the fundamental challenges of poor solubility, acidic degradation, and low oral bioavailability that have historically limited the therapeutic application of these bioactive compounds. By integrating mesoporous silica nanoparticles as a delivery vehicle with the intrinsic molecular complexity of a polyherbal matrix containing ginger, garlic, apple cider vinegar, and lemon juice, we demonstrate that the acidic environment traditionally considered detrimental can be exploited to engineer a protective steric stabilization layer through competitive adsorption.

The combined experimental-computational framework, coupling surface plasmon resonance with molecular dynamics simulations, provides a rational design principle for predicting and controlling the displacement cascades among matrix components. Our results reveal that high-molecular-weight polysaccharides from ginger and garlic, with adsorption free energies of −45.2 kJ $\text{mol}^{-1}$, thermodynamically outcompete low-molecular-weight proteins and organic acids for binding sites on the silica surface, forming a dense steric barrier approximately 5.5 nm thick. The optimized formulation,

`

prepared at pH 3.0 and 150 mM ionic strength, achieves a displacement efficiency of 0.37 ng $mm^{-2}$ and exhibits a pH-triggered release profile, with only 12.3% curcuminoid release in simulated gastric fluid compared to 78.5% in simulated intestinal fluid. The nanostabilized formulation demonstrates a 3.6-fold improvement in antioxidant potency relative to free curcuminoids, with an IC50 of 12.5 μg $mL^{-1}$.

The ablation study confirms that the complete polyherbal matrix is essential for optimal performance, with ginger polysaccharides playing the dominant role in steric stabilization. This approach offers a scalable, cost-effective alternative to conventional encapsulation methods, eliminating the need for synthetic polymer coatings or covalent surface modifications. The framework is generalizable to other complex biological media, providing a pathway for the rational design of nanoparticle-based delivery systems in traditional medicine formulations. Nevertheless, this study has several important limitations. The findings are primarily based on in vitro release, antioxidant, and surface interaction analyses, supported by computational modeling, which may not fully capture the complexity of physiological conditions in living systems. Furthermore, potential factors such as biodistribution, pharmacokinetics, long-term safety, immunological responses, and interactions with biological barriers were not evaluated in the present work.

Therefore, although the results demonstrate promising nanostabilization performance and enhanced bioactivity, they should be interpreted as a proof-of-concept rather than direct evidence of clinical efficacy. Future studies should prioritize comprehensive in vivo validation to confirm the formulation's bioavailability, therapeutic effectiveness, and safety profile under physiological conditions. In addition, long-term stability studies and the development of continuous manufacturing processes will be essential steps toward regulatory approval and eventual clinical translation.

## CONFLICT OF INTEREST

The author declares that there is no conflict of interest regarding the publication of this article. No financial, commercial, institutional, or personal relationships influenced the design, analysis, interpretation, or reporting of this study.

## REFERENCES

Bilardo, R., Traldi, F., Vdovchenko, A., et al. (2022). Influence of surface chemistry and morphology of nanoparticles on protein corona formation. Wiley Interdisciplinary Reviews: Nanomedicine and Nanobiotechnology.

Dumontel, B., Conejo-Rodríguez, V., Vallet-Regí, M., et al. (2023). Natural biopolymers as smart coating materials of mesoporous silica nanoparticles for drug delivery. Pharmaceutics.

Iranshahy, M., Hanafi-Bojd, M., Aghili, S., Iranshahi, M., et al. (2023). Curcumin-loaded mesoporous silica nanoparticles for drug delivery: Synthesis, biological assays and therapeutic potential-a review. RSC Advances.

Manzano, M., & Vallet-Regí, M. (2020). Mesoporous silica nanoparticles for drug delivery. Advanced Functional Materials.

McLean, B., & Yarovsky, I. (2024). Structure, properties, and applications of silica nanoparticles: Recent theoretical modeling advances, challenges, and future directions. Small.

Mishra, A., & Das, P. (2022). Thermodynamics of multilayer protein adsorption on a gold nanoparticle surface. Physical Chemistry Chemical Physics.

Mukhlis, L. (2025a). A Phenomenological Study of Personal Spiritual Experiences in Navigating Religious Pluralism within Interfaith Communities. *Irfana: Journal of Religious Studies*, *1*(6), 212–220.

Mukhlis, L. (2025b). Spiritual Grounds for Economic Growth: A Qualitative Exploration of Rural Indonesian Women's Transformative Journeys Through Mosque-Led Empowerment Programs. *Servina: Jurnal Pengabdian Kepada Masyarakat*, *1*(8), 289–298.

`

Mukhlis, L., & Abdullah, M. N. (2025). *Hukum Keluarga Islam di Indonesia* (1st ed.). Mukhlisina Revolution Center.

Mukhlis, L., Arifin, T., Ridwan, A. H., & Zulbaidah. (2024). Integrating Artificial Intelligenceand Maqāṣid al-Syarī'ah: Revolutionizing Indonesia's Sharia Online Trading System. *Computer Fraud and Security*, *2024*(11), 301–309. https://doi.org/10.52710/cfs.238

Mukhlis, L., Arifin, T., Ridwan, A. H., & Zulbaidah. (2025). Reorientation of Sharia Stock Regulations: Integrating Taṣarrufāt al-Rasūl and Maqāṣid al-Sharī'ah for Justice and Sustainability. *Journal of Information Systems Engineering and Management*, *10*(10s), 58–66. https://doi.org/10.52783/jisem.v10i10s.1341

Mukhlis, L., Arifin, T., Ridwan, A. H., Zulbaidah, Rosadi, A., & Solehudin, E. (2025). Reformulation of Islamic Stock Law: The Application of Taṣarrufāt al-Rasūl and Maqāṣid al-Syarī'ahto Develop a Dynamic and Sustainable Islamic Capital Market in Indonesia. *Journal of Posthumanism*, *5*(3), 1–13. https://doi.org/10.63332/joph.v5i3.913

Mukhlis, L., Janwari, Y., & Syafe`i, R. (2023). INDONESIA STOCK EXCHANGE: THEORETICAL AND PHILOSOPHICAL ANALYSIS OF MUDHARABAH AND MUSYARAKAH CONTRACTS. *Yurisprudentia: Jurnal Hukum Ekonomi*, *9*(2), 243–264. https://doi.org/10.24952/yurisprudentia.v9i2.8466

Mukhlis, L., Maryam, S., & Sormin, S. A. (2023). Model Pembelajaran Living History Berbasis PjBL Untuk Meningkatkan Keterampilan Histografi Mahasiswa. *Jurnal Educatio FKIP UNMA*, *9*(4), 1800–1809. https://doi.org/10.31949/educatio.v9i4.5595

Mukhlis, L., & Saidah, Y. (2025). Dynamics of Nature-Based learning in Developing Children's Motoricic Skills: Teacher and Parent Perspectives. *HUMANISMA: Journal of Gender Studies*, *9*(1), 64–79. http://dx.doi.org/10.30983/humanisme.v4i2.9366

Mukhlis, L., Suradi, Janwari, Y., & Syafe`i, R. (2023). Sosialisasi Saham Syariah sebagai Instrumen Pengembangan Ekonomi Masyarakat di Badan Kontak Majelis Taklim (BKMT) Kabupaten Mandailing Natal. *Jurnal Pengabdian Multidisiplin*, *3*(2), 2–9. https://doi.org/10.51214/japamul.v3i2.604

Wang, S., Wang, X., Zheng, X., Jiang, H., Liu, L., Ma, N., & Dong, X. (2025). NGR-modified curcumin nanovesicles reverse immunotherapy resistance in triple-negative breast cancer via TLR9 and mTOR pathway modulation. *Cell Biology and Toxicology*, *41*(1). Scopus. https://doi.org/10.1007/s10565-025-10055-1

Wang, Y., Sun, Y., Liu, M., Wang, C., Huang, M., Qiu, J., Yang, N., Zhang, Y., Liu, H., & Han, L. (2025). In situ and dynamic screening of extracellular vesicles as predictive biomarkers in immune-checkpoint inhibitor therapies. *Journal of Nanobiotechnology*, *23*(1). Scopus. https://doi.org/10.1186/s12951-025-03467-y

Xia, G., Fan, Z., Wang, Q., Li, J., Zhang, Y., Aipire, A., Su, Q., Li, Y., Hou, Z., & Li, J. (2025). Cascade-recharged macrophage-biomimetic ruthenium-based nanobattery for enhanced photodynamic-induced immunotherapy. *Journal of Nanobiotechnology*, *23*(1). Scopus. https://doi.org/10.1186/s12951-025-03255-8

Yang, X., Chen, W., Sun, H., He, C., Liu, Y., Qin, M., Jiang, W., Wang, Y., & He, S. (2025). Baicalin promotes anti-tumor immunity in hepatocellular carcinoma through HIF-1α/Lactate/CXCL9 axis. *Biochemical Pharmacology*, *241*. Scopus. https://doi.org/10.1016/j.bcp.2025.117157

Yuan, Z., Jiang, G., Yuan, Y., Liang, Q., Hou, Y., Zhang, W., Tang, L., Fan, K., & Feng, W. (2025). 5-FU@HFn combined with decitabine induces pyroptosis and enhances antitumor immunotherapy for chronic myeloid leukemia. *Journal of Nanobiotechnology*, *23*(1). Scopus. https://doi.org/10.1186/s12951-025-03335-9

Zhao, F., Gong, L., Wang, P., Chen, D., Cao, S., Yang, F., Tang, M., Meng, Y., Wang, Y., & Miao, L. (2025). Co-encapsulation of norcantharidin prodrugs and lomitapide in nanoparticles to regulate CCL4 expression by inhibiting Wnt/β-catenin pathway for improved anti-tumor immunotherapy. *Journal of Nanobiotechnology*, *23*(1). Scopus. https://doi.org/10.1186/s12951-025-03425-8

Zhao, W., Xu, X., An, S., Wu, J., Wang, H., Luo, J., Yuan, Y., & Li, L. (2025). Injectable PROTAC-loaded hydrogel remodels the tumor microenvironment to potentiate radio-immunotherapy. *Journal of Controlled Release*, *387*. Scopus. https://doi.org/10.1016/j.jconrel.2025.114200

.

Zhuang, L., Gao, Q., Chen, L., Xiong, X., Wei, Y., He, S., Li, D., Guan, S., & Chen, H. (2025). Catalytic immunotherapy via ultrasmall Ir supported metal clusters on defect-engineered nanoplatforms for tumor metabolic disruption and enhanced immunogenic cell death. *Nano Today*, *65*. Scopus. https://doi.org/10.1016/j.nantod.2025.102878

Nie, W., Zhang, X., Kang, P., Lan, J., Li, Z., Gu, D., Zhou, R., et al. (2025). Exploring the influence of polysaccharide on gastrointestinal stability, drug release and formation mechanism of nanoparticles in zhimu and huangbai herb pair …. Scientific Reports.

Shen, L., & Ji, H. (2025). Regulation of gut microbiota by ginger, its derived polysaccharides, essential oils, gingerols, and shogaols and related health outcomes. Food Chemistry.

Yan, X., Feng, Z., Wang, X., Yu, H., Liu, F., & Liu, W. (2025). Panax quinquefolium l. Polysaccharide-protein conjugated nanoparticle stabilized pickering emulsion: Structural characteristics, in vitro digestive stability, and its …. Food and Bioproducts Processing.

Yang, H., Wang, S., Yang, L., & Liu, H. (2024). Preparations, application of polysaccharide-protein nanoparticles and their assembly at the oil-water interface: Preparation and application of PPNPs. Food Science and Biotechnology.

Yardımcı, B. (2023). Spectrophotometric and smartphone-based facile green chemistry approach to determine nitrite ions using green tea extract as a natural source. Sustainable Chemistry and Pharmacy.

Yiasmin, M., Azad, S. A., Easdani, M., et al. (2026). The state-of-the-art on exploring polysaccharide-protein interactions and its mechanisms, stability, and their role in food systems. Food Reviews International.